Robust analysis and control of an inverted pendulum

Lihao Liu

I. Introduction

The inverted pendulum on a cart is a classic educational project in control engineering, yet it has significant parallels with various practical systems, including Segways, cranes, and rockets. Analyzing this system can provide important insights into addressing similar challenges in these applications. This project aims to design and implement a controller for such systems, with the specific objective of tracking a reference velocity while maintaining an upright orientation with respect to the horizontal plane. Additionally, the controller must be able to handle uncertainties and disturbances, ensuring robust performance under varying conditions and model uncertainty.

In particular, to ensure that our analysis is grounded in reality, we will focus on the dynamics of a two wheeled Segway operated by a human rider, as real world data is readily available for Segways. Actuators and sensors have also been modelled by referencing real world commercial motors and sensors. This approach enables us to perform simulations that accurately reflect the practical conditions and constraints encountered in actual Segway systems, while still been providing insights about the more general problem of the inverted pendulum on a cart. For references about the numerical values of the data, see [1], [2], [3], [4].

II. Literature review

The problem of stabilizing an inverted pendulum has been extensively studied in control theory due to its fundamental importance and its practical applications in various domains, including robotics, aerospace, and transportation systems. Numerous studies have focused on different configurations and control strategies for inverted pendulum systems. However, the specific problem we aim to tackle, controlling the velocity of a cart while maintaining the pendulum in an upright position, has not been comprehensively addressed in the existing literature.

A. Existing research on inverted pendulum systems

Most of the research on inverted pendulum systems can be categorized into two main configurations: the inverted pendulum attached to a fixed point and the inverted pendulum on a movable cart. In the first configuration, a torque is applied at the pivot point to keep the pendulum upright. Various control strategies, such as Proportional-Integral-Derivative (PID) control, Linear Quadratic Regulator (LQR), and nonlinear control methods, have been employed to achieve stabilization in this setup [5] [6].

In the second configuration, the pendulum is mounted on a cart that can move horizontally. The control objective is typically to keep the pendulum upright by adjusting the cart's position. This setup has been extensively studied, with many researchers applying linear and nonlinear control techniques, including State-Space control, Fuzzy Logic Control (FLC), and Sliding Mode Control (SMC) [7] [8]. These studies have shown effective stabilization of the pendulum by controlling the cart's position.

B. Gap in the Literature

Despite the extensive research on these configurations, there is a notable gap in addressing the combined problem of controlling both the velocity of the cart and the angle of the pendulum. Most existing studies focus solely on stabilizing the pendulum without considering the need to control the cart's velocity. This new problem presents some unique challenges, as it requires maintaining the pendulum in an upright position while simultaneously ensuring the cart tracks a specified speed.

C. Our approach

Our project aims to fill this gap by developing a control strategy for an inverted pendulum on a cart, where the cart is required to track a certain speed while maintaining the pendulum upright. This problem is particularly relevant for applications such as the Segways or cranes.

III. Modelling of the open loop system

In the following sections, we model our open loop system, where the Segway is represented as an inverted pendulum on a cart. The inverted pendulum represents a human driver, while the cart represents the wheels of the Segway. The wheels are driven by a DC motor that applies force to move the cart forward or backward. Another DC motor provides torque to the pendulum to assist in maintaining its upright position. The dynamics of the sensors are neglected in this initial modeling and will be addressed later in the uncertainty analysis.

A. Inverted pendulum on a cart

Consider figure 1, the following equations are the sum of all the forces in the x axis direction and the sum of all the torques in the z axis direction with respect to the fulcrum of the pendulum:

$$\begin{cases} (M+m)\ddot{x} = ml\dot{\theta}cos\theta + ml\dot{\theta}^2 sin\theta + F \\ (I_{CM} + ml^2)\ddot{\theta} = mglsin\theta + ml\ddot{x}cos\theta + T \end{cases} \tag{1}$$

This is a highly non linear system and its equilibrium points are $\theta = k\pi, \quad k \in \mathbb{N}$.
Linearizing around $\theta = 0$ with the small angle approximation we obtain:

$$\begin{cases} (M+m)\dot{v} = ml\dot{\omega} + F \\ I\dot{\omega} = mgl\theta + ml\dot{v} + T \end{cases} \tag{2}$$

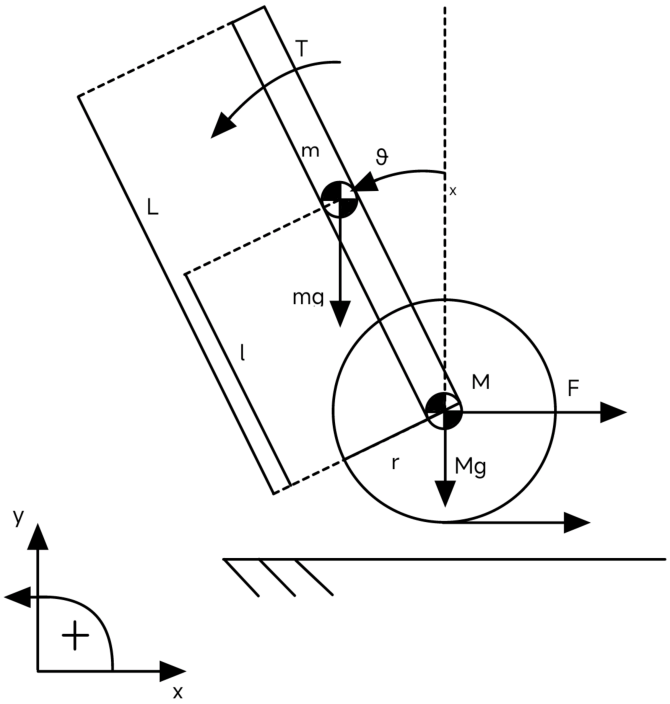

Fig. 1. Inverted pendulum on a cart system

Where $I = I_{CM} + ml^2$, $v = \dot{x}$ and $\omega = \dot{\theta}$. By denoting $q = (M+m)I - m^2l^2$, the transfer function representation of the inverted pendulum on a cart is then:

$$G(s) = \begin{bmatrix} G_{11}(s) & G_{12}(s) \\ G_{21}(s) & G_{22}(s) \end{bmatrix} \tag{3}$$

$$G_{11}(s) = \frac{Is^2 - mgl}{qs^2 - (M+m)mgls} \tag{4}$$

$$G_{12}(s) = \frac{mls}{qs^2 - (M+m)mgl} \tag{5}$$

$$G_{21}(s) = \frac{ml}{qs^2 - (M+m)mgl} \tag{6}$$

$$G_{22}(s) = \frac{M+m}{qs^2 - (M+m)mgl} \tag{7}$$

]

B. Actuators

From [9] the equations of a permanent magnet DC motor can summerised as:

$$V = L_a \frac{di}{dt} + R_a i + K\omega_{motor} \tag{8}$$

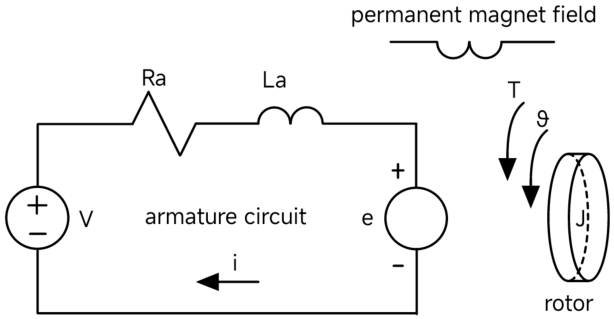

Fig. 2. DC motor scheme

$$T_{motor} - T_{load} = J\frac{d\omega_{motor}}{dt} + B\omega_{motor} \tag{9}$$

The terms $K\omega_{motor}$, $J\frac{d\omega}{dt}$ and $B\omega_{motor}$ can be negleted because of their small value. The effect of ignoring them will be taken into account in our uncertainty analysis. This results in the following transfer function:

$$\frac{F_{load}}{V}(s) = \frac{K}{L_a(s + R_a/L_a)} \tag{10}$$

IV. Coupling of the actuators with the system

The force and torque provided by the motors is transmitted to the system through a gear ratio n and wheels of radius r:

$$A_1(s) = \frac{F}{V1} = \frac{K}{rnL_a(s + R_a/L_a)} \tag{11}$$

$$A_2(s) = \frac{T}{V2} = \frac{K}{nL_a(s + R_a/L_a)} \tag{12}$$

A. Scaling

All the transfer functions have been scaled by values related to the their inputs and outputs. In the case of the system transfer functions, we used the maximum expected input and maximum allowable error of the output. In the case of the actuators, the maximum expected input and maximum allowable output were used. Let $H(s)$ be a generic transfer function.

$$H(s)_{scaled} = H(s)\frac{input\ scaling}{output\ scaling} \tag{13}$$

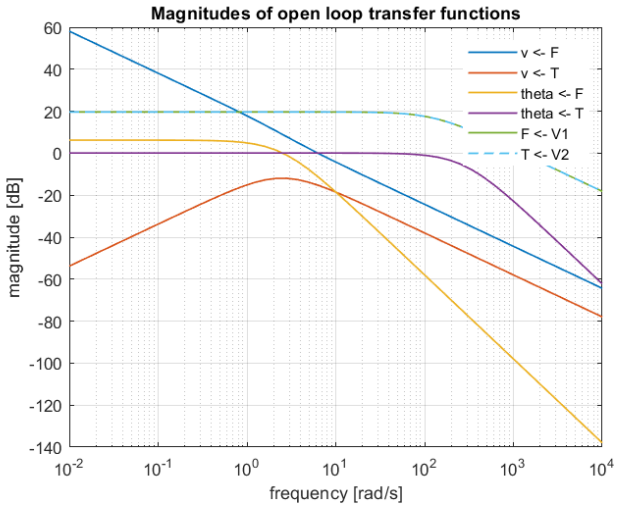

Fig. 3. Magnitude plots of the systems scaled transfer functions

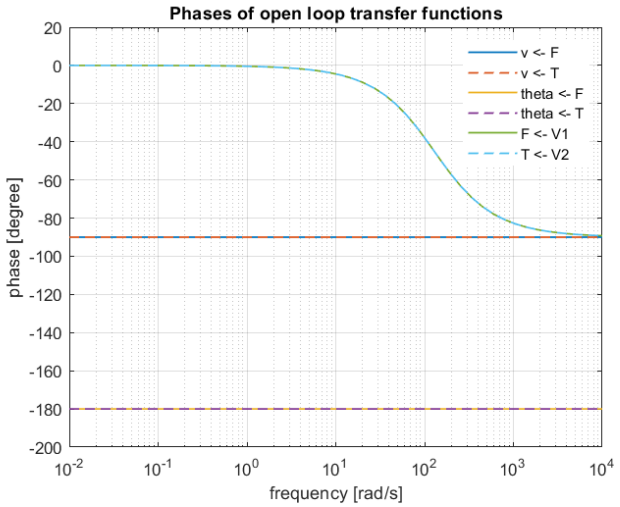

Fig. 4. Phase plots of the systems scaled transfer functions

Fig. 3 and fig. 4 show the bode plots of the systems transfer functions after scaling. Except for the actuators, the bandwidth of the inverted pendulum is in the range $[1,\ 100]\,rad/s$, so we will focus our following plots around the range $[0.01,\ 10000]\,rad/s$. Notice also how the transfer functions to the torque (fig. 4) have a constant phase of -180 degrees.

B. Nominal open loop system

Denoting with $A(s)$ the MIMO transfer function containing in its diagonal the actuators transfer function, the nominal open loop system can be represented by the product of $A(s)$ and $G(s)$

$$\begin{bmatrix} v \\ \theta \end{bmatrix} = G(s)A(s) \begin{bmatrix} V_1 \\ V_2 \end{bmatrix} \tag{14}$$

Where V_1 and V_2 are the armature voltage of the force actuator and the torque actuator respectively.

While the actuators are stable, with poles in $p = -\frac{R_a}{L_a} < 0$, the dynamics of the pendulum is highly unstable. Fig 5 shows the response of the angle θ to a unit impulse torque T.

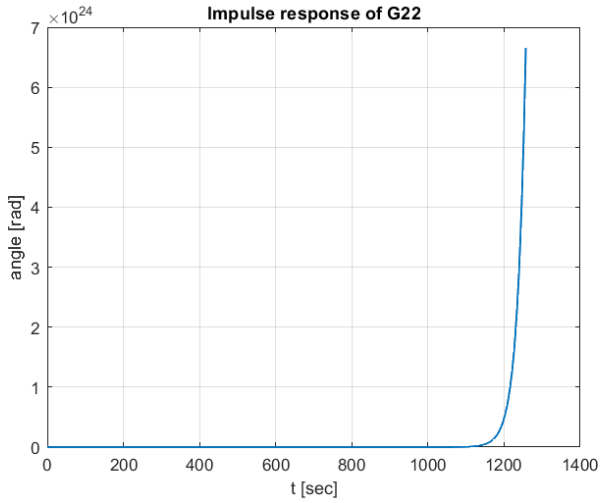

Fig. 5. Response of the angle to a unit impulse in the torque

V. Nominal controller

We now synthesize a controller for the nominal system using `hinfsyn` from MATLAB. First the generalized plant model was derived by building the open loop plant in Simulink, comprehensive of performance weights and uninitialized uncertainty weights, then *hinfsyn* is called on the nominal plant with `nmeas = 4` and `nctrl = 2` as the controller receives 4 signals and sends 2 signals, respectively: reference v, reference θ, measured v, measured θ, force actuator's voltage $V1$, torque actuator's voltage $V2$.
The performance weights for the actuators were chosen to be high at high frequencies to prevent spikes in the force and torque values in response to sudden changes in reference signals. The measurement noise weights were selected based on the bandwidth and noise data found in the relevant references, [3] and [4]. Fig. **??** shows the magnitudes of all weights.

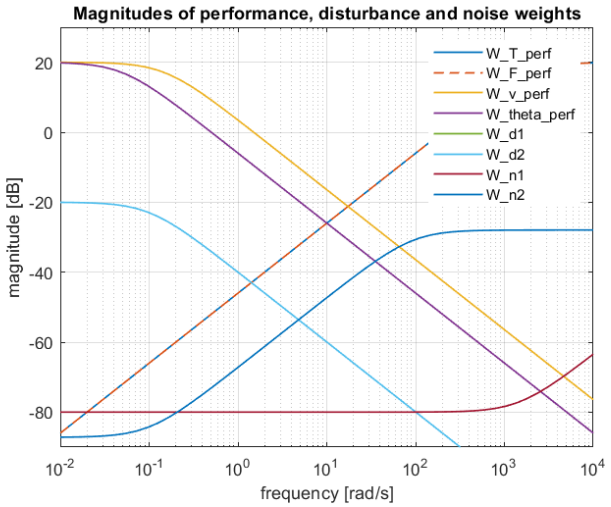

Fig. 6. Magnitude plots of performance weights and disturbance and noise dynamics

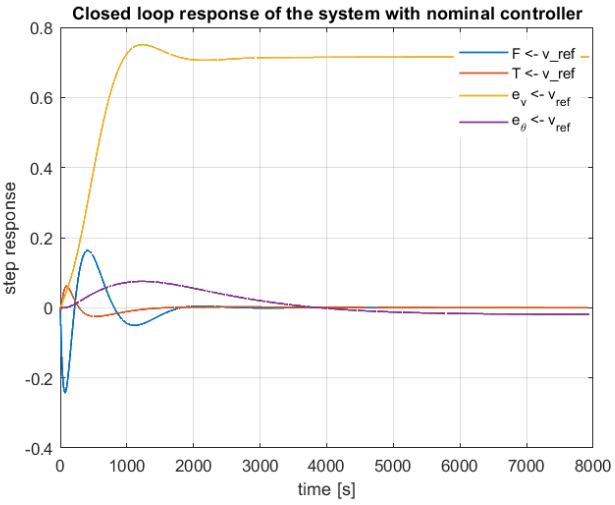

Fig. 7. Closed loop response of F, T, e_v and e_θ

Fig. 7 shows the response of F, T, e_v and e_θ in response to a step input to the reference velocity. All the values are bounded, showing the stability of the closed loop system. Given our initial scaling of the transfer functions, having a steady state error on the velocity e_v of 0.7 means that our steady state error never exceeds our allowable maximum error, showing also a good performance in the tracking of our references.

VI. Uncertainties

Our system is inherently subject to uncertanties, wheter due to approximations in our models, unaccounted noises and disturbances, or even errors in the datasheets from which we got our numerical values. To ensure stability and good performance even in uncertain situations, we augment our model with uncertainty modelling and will later try to synthesize a robust controller that is able to perform well even in the worst case scenario. The uncertainty weights have all been implemented using the function $makeweight$ from MATLAB. Generally it has been observed that uncertainties are higher at higher frequencies, particularly for sensors. Therefore, all uncertainties have been increased by at least one order of magnitude at higher frequencies to ensure robustness.

A. Uncertainty from the DC motors approximated model

In the modelling of the DC motors, we ignored the effects of $K\omega_{motor}$, $J\frac{d\omega}{dt}$ and $B\omega_{motor}$. Although their values might be very small, in reality they still have an effect on the performance of the actuators. To take this into account, we decide to have an uncertainty in the actuator's output of 0.15% that rises to 1% at high frequencies.

B. Uncertainty from sensor datasheets error

The noise on our measurements was modelled by referencing the datasheets of real world sensor, but even manufacturer datasheets can contain errors. According to [3] and [4], the velocity sensor and the angle sensors are incredibly precise, so even an uncertainty weight in the measurements of just 0.1% that rises to 10% at high frequencies is enough to upper bound all possible uncertainties.

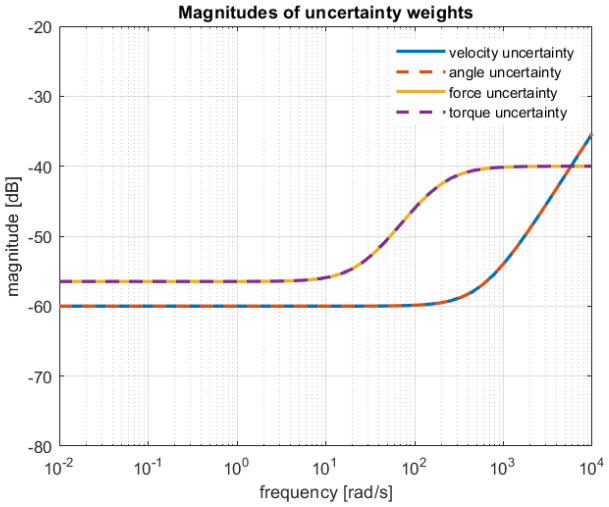

Fig. 8. Magnitude plots of the uncertainty weights

VII. μ ANALYSIS AND CONTROL SYNTHESIS

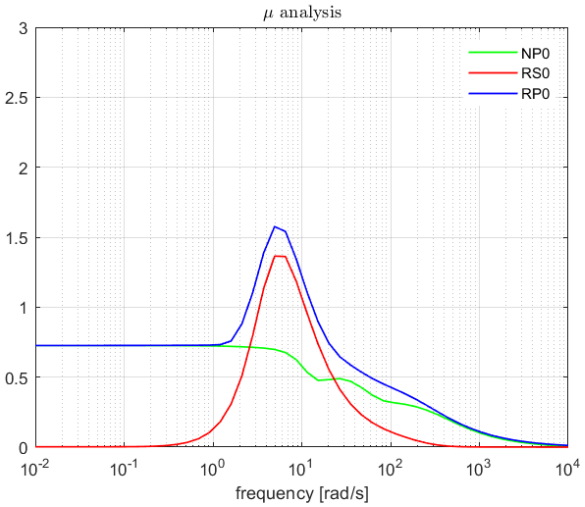

Fig. 9. μ analysis: first iteration

Fig. 9 shows the μ analysis [10] using the nominal controller. The nominal performance is below 1 for all frequencies, but the robust stability and robust performance have problems in the range of frequencies $[1, 100]$, reaching values of around 1.5. This means that with our nominal controller, we can provide robust stability and robust performance for uncertainties of norm up to $\frac{1}{1.5}$. We now try to find a controller that performs better in conditions of uncertainty by performing the DK iteration process [10]. From `mussv` we obtain `muinfo` from which we extract the D scaling matrices. Fig. 10 shows the fitting of only of the elements in the D matrix.

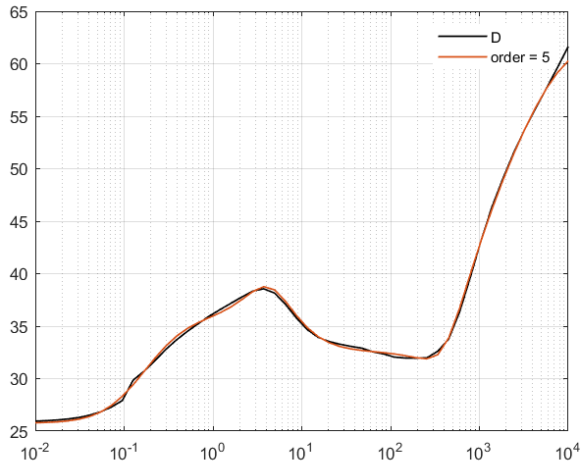

Fig. 10. Fitting of an element of scaling matrix D using an approximated system of order 5

By fitting these numeric matrices with transfer functions that approximate them using `fitmagfrd`, we synthesize a new controller $K1$ and perform the μ analysis again. The result is show in fig. 11

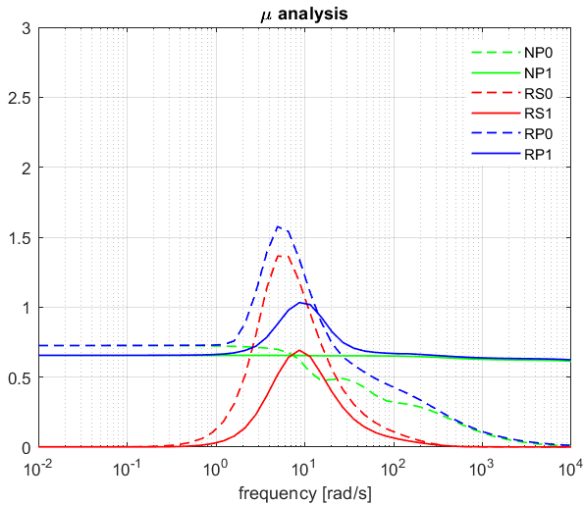

Fig. 11. $\mu analysis$: second iteration

This time both the robust stability is below the unit value, while the robust performance is just around the unit value. Only one iteration of the DK process was needed. The nominal performance however has generally become worse compared to the nominal plant, especially at higher frequencies.

VIII. CLOSED LOOP SIMULATION OF ROBUST CONTROLLER

We now compare our previously found nominal controller with the new robust controller in the worst case scenario of a pertubed plant. The theory tells us that since the nominal controller does not manage to achieve a structured singular value below 1, the resulting closed loop system with the worst case pertubed plant will be unstable, while the robust controller should be able to handle it.

The following figures show the responses of the actuators and the errors of the tracked variables when our system receives a step input for the velocity reference and the angle references is kept at zero.

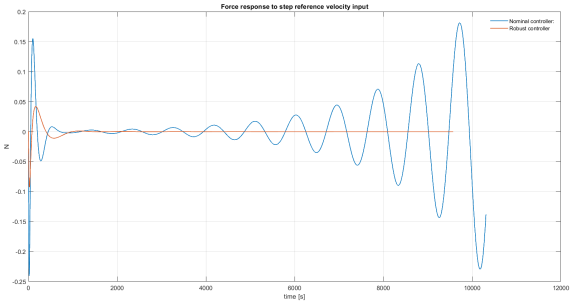

Fig. 12. Force responses to a step reference velocity input

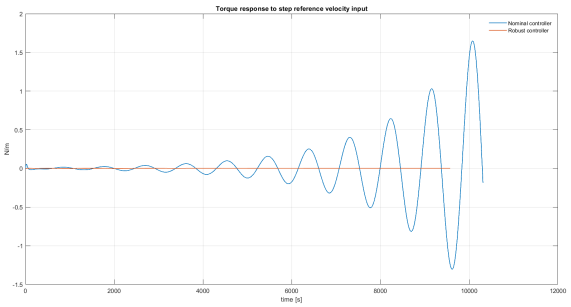

Fig. 13. Torque responses to a step reference velocity input

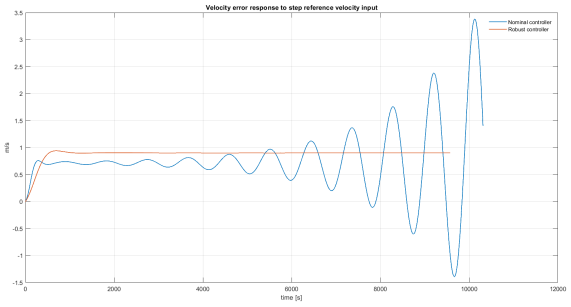

Fig. 14. Velocity error responses to a step reference velocity input

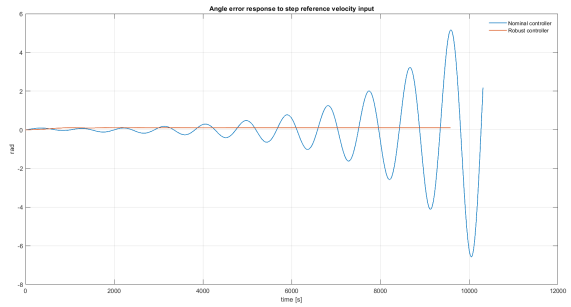

Fig. 15. Angle error response to a step reference velocity input

As can be seen from all the figures 12, 13, 14 and 15, the responses with the nominal controller tend to oscillate and diverge progressively. The responses with the robust controller on the other hand remain stable and reach a finite steady state value. This show that the nominal controller has neither robust stability nor robust performance, which is instead achieved by the robust controller designed with DK iteration.

Similar to our simulation of the nominal plant with the nominal controller in fig. 7, in the case of the pertubed plant with robust controller the actuator outputs quickly decay to zero. The errors of our tracking variables never go above the unit value, this means that the error never exceed their allowable maximum values.

The results of our simulations confirm the theory and are in line with our μ analysis.

IX. Conclusion

We have build a basic model for an inverted pendulum on a cart with actuators and sensors, employing actual data obtained from a Segway for our simulations. Initially, we found a nominal controller capable of stabilizing the system and enabling reference velocity tracking. However, subsequent analysis revealed its non robustness to perturbations. To address this, we synthesized a robust controller through DK iteration, demonstrating its effectiveness even under the worst case perturbation. While we have been mainly referencing Segways, it should be noted that our results are applicable to a broader set of systems that share similarities to the general model of an inverted pendulum on a cart.

References

[1] Segway, "Segway pt i2 and x2 product brochure," https://www.segway.ch/en/infos/technologie.php, n.d., accessed: 2024-05-31.

[2] Kollmorgen, *SRF3736-4983-84-5-56BC-CU DC Motor Datasheet*, Kollmorgen Permanent Magnet DC Motor Selection Guide, n.d., accessed: 2024-05-31.

[3] Honeywell, *SNDH-H Series Hall-Effect Speed Sensor Technical Manual*, https://sensing.honeywell.com/hall-effect-speed-sensors-sndh-series, n.d., accessed: 2024-05-31.

[4] Silicon Sensing, "Crm100 technical datasheet," https://www.siliconsensing.com/products/crm100/, n.d., accessed: 2024-05-31.

[5] K. J. Åström and K. Furuta, "Swinging up a pendulum by energy control," *Automatica*, vol. 36, no. 2, pp. 287–295, Feb 2000.

[6] D. J. Block, K. J. Åström, and M. W. Spong, *The reaction wheel pendulum*, ser. Synthesis Lectures on Control and Mechatronics. Morgan & Claypool Publishers, Feb 2007, vol. 1, no. 1.

[7] R. Tedrake, T. W. Zhang, H. S. Seung, and S. C. Tallamraju, "Learning to walk in 20 minutes," in *Proceedings of the Fourteenth Yale Workshop on Adaptive and Learning Systems*, New Haven, CT, USA, June 2007, pp. 193–199.

[8] G. Campa and M. Napolitano, "Sliding mode control of an inverted pendulum with cartesian motion," *IEEE Transactions on Aerospace and Electronic Systems*, vol. 33, no. 3, pp. 1000–1015, July 1997.

[9] L. Zaccarian, "Dc motors: dynamic model and control techniques," 01 2005.

[10] S. Skogestad and I. Postlethwaite, *Multivariable feedback control: Analysis and Design*. Hoboken, US-NJ: John Wiley, 2005.